Elaboration of a hydrogeological conceptual model by application of electrical resistivity tomography: Case of the Lobo catchment (Centre-Western Côte d'Ivoire)

Jean Olivier Kouadio Kouamé, Jules Mangoua Oi Mangoua, Abe Parfait Sombo, Frédéric Paran, Brou Dibi, Didier Graillot

Elaboration of a hydrogeological conceptual model by application of electrical resistivity tomography: Case of the Lobo catchment (Centre-Western Côte d'Ivoire)

KOUADIO Kouamé Jean Olivier[a,b*], MANGOUA Oi Mangoua Jules[a], SOMBO Abe Parfait[a], PARAN Frédéric[b], DIBI Brou[a] and GRAILLOT Didier[b]

[a]Laboratoire des Sciences et Technologies de l'Environnement, Université Jean Lorougnon Guédé, BP 150 Daloa, Côte d'Ivoire;

E-Mail: olivierkouame05@gmail.com

[b]UMR 5600, École Supérieure des Mines de Saint-Étienne, 158 cours Fauriel, 42023 Saint-Étienne, France

E-Mail: graillot@emse.fr

Author to whom correspondence should be addressed; E-Mail: olivierkouame05@gmail.com

Tel : +33 6 05797156/ +225 0707162425

Abstract

Drinking water supply in the Lobo catchment is based mainly on surface water. In recent years, the adverse effects of climate change and strong population growth have led to increasing uncertainty about the availability of surface water and growing interest in groundwater in this region. Therefore, to ensure sustainable management of this resource, it is necessary to characterise and understand this groundwater system. This characterization requires knowledge of the geometry and structure of this aquifer system, which is a prerequisite for ensuring future water supply from groundwater resources. This aquifer system, which is the subject of this study, has never been the subject of a study aimed at characterising it and getting to know it better. This study aims to improve the knowledge of this aquifer system by elaborating the geometry of this aquifer system through the study of drilling data and electrical resistivity tomography (ERT). The results show that weathering of the granitic rocks in the Lobo catchment leads to the development of composite aquifers at two levels: a shallow saprolite aquifer overlies in places by a thick layer of ferruginous crust, and a deeper and very thick fractured aquifer. This shallow weathering aquifer, fed directly by precipitation, is tapped by conventional large diameter wells that are generally not immune to seasonal fluctuations. For sustainable management of this resource, an assessment of its recharge should be undertaken in addition to this study of the geometry of this aquifer system. The results of this study of the geometry of the Lobo catchment aquifer system improved the understanding of this aquifer system and will assist in groundwater exploration in this area.

Keywords: Fractured aquifer, Lobo catchment, Climate change, Saprolite, Electrical resistivity tomography

Introduction

Water is an essential element, indispensable for life, for natural ecosystems and an undeniable socio-economic asset [1]. It is source of life and the most important factor in achieving sustainable development. However, in developing countries such as Côte d'Ivoire, access to this resource is not always guaranteed due to the negative impact of climate change [2]. In Côte d'Ivoire, the bedrock is

97.5% crystalline rock. Therefore, the drinking water supply of large cities is generally provided by large surface water bodies. Due to their low productivity, groundwater from these crystalline bedrock aquifers is generally used to meet the water needs of the rural population [3, 4]. However, in the context of the climate change negative impacts, these geographically well distributed aquifers [5] have been used in recent years as an alternative source of water in several major cities in Côte d'Ivoire.

Daloa, the third largest city in Côte d'Ivoire and the economic center of the Lobo catchment area, has experienced problems with access to drinking water. Indeed, the reservoirs built at Lobo River for supplying drinking water to the major cities, is subject to numerous anthropogenic pressures. For example, Vavoua, the second largest city in the area, has abandoned its water reservoir at Lobo River due to advanced eutrophication and has turned to groundwater resources [6]. Therefore, the drinking water supply for the population in this area is currently provided by several drillings. To compensate for the recurrent water supply problems in Daloa, the authorities are considering using groundwater as an alternative source to improve the drinking water supply in this town and its surroundings. For sustainable management of this resource and to improve the success rate of drilling in the area, a detailed knowledge and understanding of groundwater dynamics and key hydrogeological processes is required [7]. [8] have shown that the main cause of drilling failure in crystalline rocks is weak understanding of the aquifer system. According to [9], the hydrogeology of bedrock aquifers is highly dependent on the overall evolution of weathering, its depth and spatial distribution. The thickness and lateral extent of the weathered zone that control the storage capacity of this aquifer system and the yield of wells in this zone depend mainly on the available saturated thickness. In weathered zones, where the original texture of the source rock is completely destroyed, and which generally have low porosity, the yield of these aquifers is low. However, the presence of fractured zones enhances the storage and flow of groundwater, generally received through the overlying weathered zone. In these areas, fractures and vertical joints immediately beneath the weathered zone generally convey water to a deeper fracture network that controls the movement and direction of groundwater flow [10].

However, no studies have been conducted in Lobo catchment to characterise this aquifer system and understand the various hydrogeologic processes. Basic information such as the geometry of the underlying aquifer is required for planning sustainable groundwater management strategies in the Lobo catchment [11]. In this regard, geophysical surveys such as electrical resistivity tomography (ERT) and information from drilling logs in the area, may be important [12,13]. Electrical resistivity tomography (ERT) is an effective tool for studying the hydrogeological properties of the subsurface [14]. This technique is not only provides the geological structure but, in addition, it can reveal information about possible groundwater occurrence. The applications of this technique, which has

been used for many years, have increased due to advances in data acquisition techniques, and computer technology for their processing [14]. Therefore, it has become more accurate and efficient to map the complex and small-scale geological features [15]. Geophysics, especially electrical resistivity tomography (ERT), is a highly recommended tool for groundwater prospecting in crystalline bedrock [16]. This technique can be used to determine the exact location of geological discontinuities with greater accuracy and locate areas of high hydrogeological interest [16,17]. In addition, this technique can be successfully used to characterise areas of weathered rocks, as a pronounced contrast can be clearly observed when fresh rocks are reached [14]. In the Lobo catchment, this technique has never been used to characterise this aquifer system.

The objective of this work is to use electrical resistivity tomography (ERT) data to characterise the geometry of the aquifer in this area and validate this geometry using drilling data. The geometry of this aquifer system to be characterise can contribute to the creation of a conceptual model that can be used to develop a sustainable management plan for this resource.

Study area

Lobo catchment area is located in central-western Côte d'Ivoire, between 6°05' and 6°55' west longitude and between 6°02' and 7°55' north latitude. This area is bordered by the regions of upper Sassandra, of which Daloa is the regional capital, and part of Worodougou (Séguela). The catchment area has a surface area of 7,000 km². It is drained by the Lobo River and its main right tributary, the Dé. The average rainfall during 1971-2016 is about 1,330 mm/year and the average temperature is 25°C. The population is estimated at about 1 million inhabitants, with an annual growth rate of 3.1% [18] of which 49% live in the department of Daloa. The drinking water supply for the population of the catchment is provided by both surface water and groundwater. The geological formations of the Lobo basin belong mainly to the Precambrian basement and are divided into two main groups: igneous rocks, which consist mainly of granite, and metamorphic rocks, which consist of shale. Granitic rocks cover about 95% of the area [19] (Fig. 1).

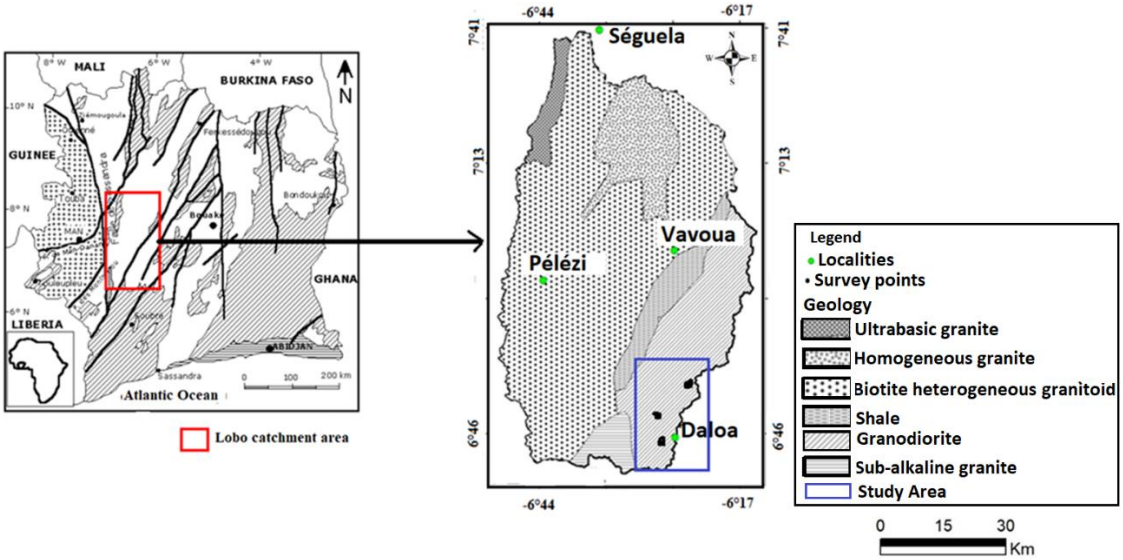

Fig.1. Geological formations of the Lobo catchment

Material and Methods

The sites investigated in this study were selected after preparatory work. As a first step, a campaign to collect drilling logs was organized and an interpretation of aerial photographs of the area was made. Then, field visits were organized to get an idea of the geomorphology, weathering profile at the outcrops in the area and the condition of the existing boreholes. Finally, 1D electrical surveys were carried out and an analysis of these results was undertaken to select points for ERT surveys.

Drilling data were collected by the Territorial Directorate of Human Hydraulics (DHH) based in Daloa (capital of the region of upper Sassandra). These data were obtained from the analysis of 315 villages and urban files. Of the 315 drillings data sheets that existed prior to this study, only 159 boreholes have complete data. As a result of the study, 16 new wells were drilled and their data sheets were also used to improve our analyses. A total of 159 drillings data sheets were used in this study (Fig. 2).

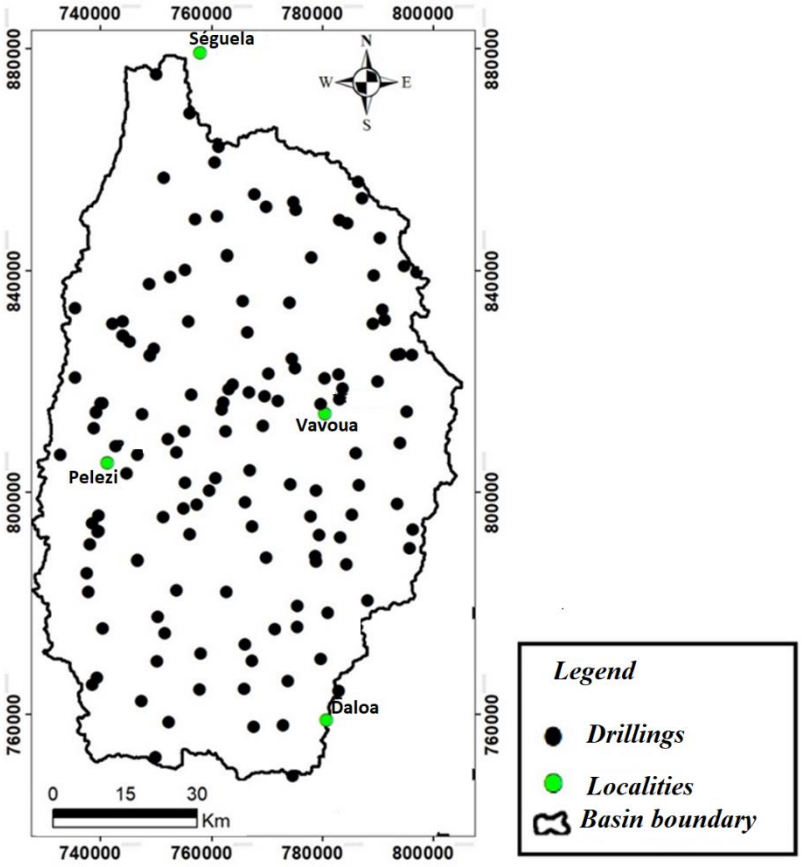

Fig.2. Drillings location of the Lobo catchment

The methodological approach used in this study consisted first of analysis of the lithologs and cuttings, to determine the nature and thickness of the differents layers of the weathering profile and the lithology of the parent rock. Then, vertical electrical soundings (VES) were carried to determine the different electrical resistivities of the main geological formations. Finally, 2D electrical resistivity tomography (ERT) sections were determined and geologically classified based on the corresponding layers of the weathering profile derived from the electrical logs.

The elaboration of the structure of the weathered zone was based initially on the interpretation of 159 logs from old boreholes and secondly on the interpretation of the electrical logs recorded in the 16 new unequipped drillings. The interpretation of these lithologs was improved by the use of additional drilling data (drilling rate and change of drilling tools) and outcrop observation. Drill cuttings were examined to assess the nature and geometry of the various components of the weathering profiles corresponding to the geological formations in the catchment.

Electrical resistivity methods are used as described in [20]. These methods consist of injecting a direct current into the soil with electrodes A and B and measuring the difference in electrical potential between the other two electrodes M and N. In this study, Schlumberger array configuration was used for the vertical electrical soundings (VES), with a maximum electrode spacing (AB/2) 200 m. All measurements were made with SYSCAL Pro. The location of the VES was based on the information available from the drillings logs of the different sites surveyed [21]. This is to

quantify the thickness and resistivity of different layers of this aquifer system. The values of apparent resistivity (ρa) obtained from the survey are estimated as follows (equation 1) [20]:

$$\rho_a = \pi \frac{[(AB/2)^2 - (MN/2)^2]}{MN} \quad \frac{V}{I} \qquad (1)$$

Where:

ρ_a: the apparent resistivity in Ω.m,

V: the difference of potential in volts (V) measured between the potential electrodes,

I: the applied current strength in ampere (A).

AB: the distance between current electrodes in meters (m),

MN: the distance between potential electrodes in meters (m).

The interpretation of sounding data is done with the software IPI2Win.

Wenner, Schlumberger, pole-pole, dipole-dipole and pole-dipole arrays are the most commonly used for 2D resistivity measurement. In this study, the pole-dipole arrays has been used for differentiating complex geological structures [22]. The pole-dipole array was used because it has much higher signal strength to obtain high resolution of 2D ERT data, as well as higher vertical sensitivity and great depth of investigation [23]. The multi-electrode resistivity technique uses multi-core cables (SYSCAL-Pro from Iris instrument) with as many conductors as electrodes plugged into the ground at fixed spacing. The SYSCAL-Pro was coupled with two (2) or four (4) electrical cables depending on the depth of interest. In this study, two sets of profile lengths (240 m and 480 m) were applied depending on the availability of lateral space for deployment of the required cable length. For a 240 m profile investigation, two (2) cables of length 120 with minimum takeout separation of 2.5 m were connected on either side of the SYCAL-Pro along a chosen direction. On the other hand, for a 480 m traverse investigation, four (4) cables each of length 120 m with minimum electrode takeout of 5 m were connected on the flip side of the resistivity meter. A total of 96 electrodes were used with an electrode at infinity (1 km). This configuration was chosen for the study to increase the depth of the cross-sections [24]. Fig.3 shows the different sites surveyed. RES2DINV software [25] was used to invert the apparent resistivity values into a resistivity model section. The least-squares fitting technique [26] was used to obtain the best fit for the resistivity model. A series of iterations were performed until the difference between the model response and the measured data was minimal. This difference is quantified in terms of a root mean squared error value (RMS) (equation 2).

$$RMS = \sqrt{\frac{\left(\sum_{i=1}^{n}(x_{data,i} - x_{model,i})^2\right)}{\frac{x_{data,i}}{N}}} \quad (2)$$

where N represents the total number of measurements,

x_{data} : field data,

x_{model} : simulated data

However, as it has been shown that low values of RMS do not guarantee that the model provides an accurate representation of the subsurface [27], it is still important to refer to lithologs when calibrating geophysical data. The geophysical models obtained by inversion were clustered according to the resistivity ranges [28] corresponding to the saprolite, fractured and fresh rock layers determined from the electrical resistivity logs.

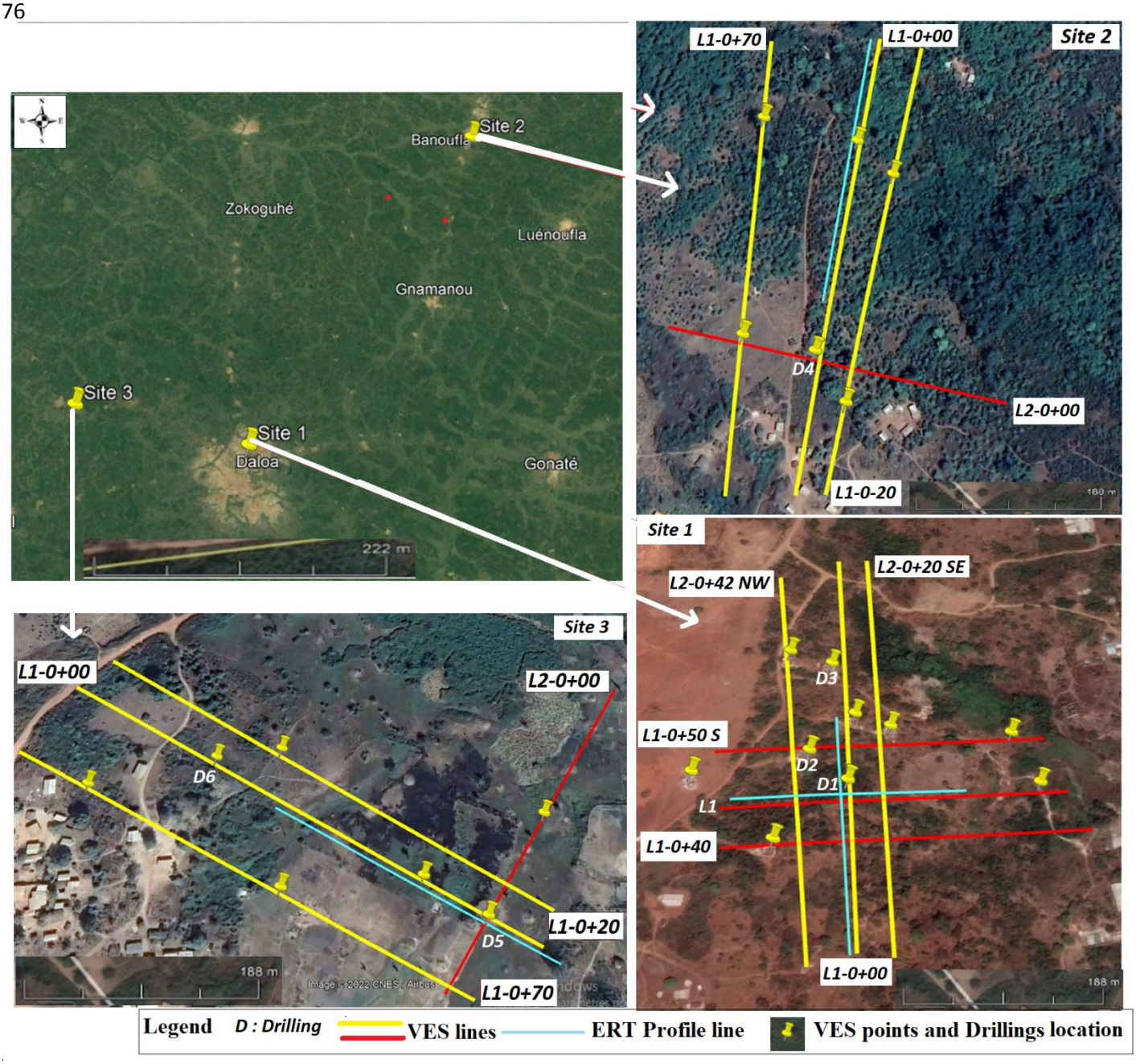

Fig. 3. View of the different surveyed sites with some VES points, drillings and ERT profile lines

Results

Lithostratigraphic description

The analysis of the 159 lithologs shows that the weathering profile of the Lobo catchment corresponds to a classical horizontal structuring. The analysis of these different sections revealed a general heterogeneity between the different profiles. However, four different horizons can be deduced from these profiles. Thus, the topsoil is the identified surface horizon, its thickness varies from 0 to 1.5 m and can be up to 2.5 m. It is usually located above the saprolite layer. The lithological structure of our study area, from top to bottom, is as follows:

- ✓ **The ferrous crust**: ferruginous in its upper part and clayey in its lower part. It is not always visible at the outcrop, but has a thickness that varies between 4 and 5 m and can be up to 10 m. It covers the saprolite layer. When this layer is exposed, it reduces the penetration of water into the ground.
- ✓ **The Saprolite layer:** it can be divided into two sublayers. The alloterite sublayer (rich in clay) and the isalterite sublayer (rich in sand). The average thickness of the saprolite is 35 m and varies from 18 to 58 m in depth. The alloterite layer has an average thickness of 21 m, but can reach 40 m. It is generally composed of lateritic clay with some sand grains, but the fresh rock is not evident in this layer. The isalterite layer has an average thickness of about 10 m, but can reach 28 m. It generally consists of fine and coarse sand; clayey sand and sometimes highly weathered granite.
- ✓ **The Fissured layer**: it lies between the fresh rock and the isalerite sublayer and in wich most of the water inflow is observed. This layer is characterised by cuttings containing both weathered and fresh rock elements. The thickness of this fracture layer generally ranges from 25 to 80 m with an average of about 65 m. In the Lobo River catchment, this layer consists mainly of slightly weathered granite (Fig.4).
- ✓ **The Fresh rock:** located underneath the weathering profile, this layer may be visible at the outcrop. It is permeable only where deep fractures are present. Even when these fractures are as permeable as the fractures of the fissured layer, their density is less at depth and laterally. It is generally composed of granitoids. Although this structure is typical of granitic rocks, there are sometimes marked differences in thickness depending on the topography.

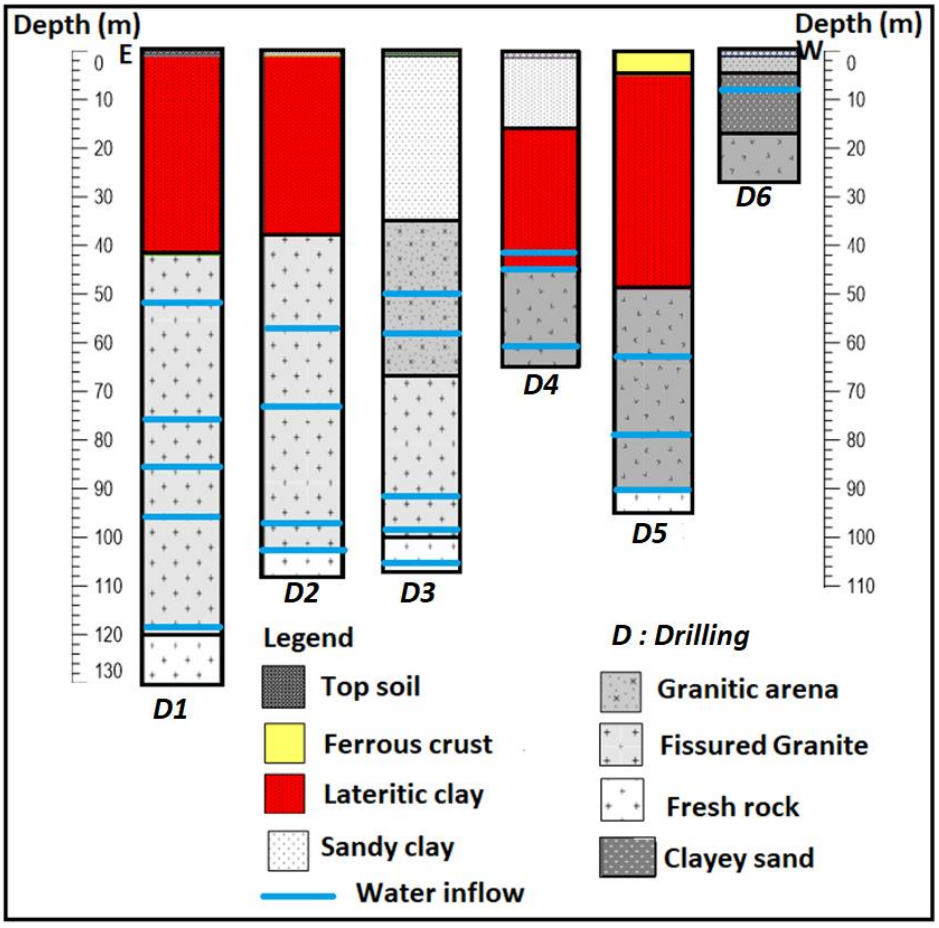

Fig. 4. Weathering profiles on granite in the Lobo catchment. The height of the ferrous crust is about 4 m.

Interpretation of electrical resistivity logs

Vertical electrical soundings (VES) carried out over the study area with a distance (AB/2 = 200 m) show a variation of electrical resistivity with depth (Fig.5). These vertical electrical surveys allowed us to identify 2 or 4 geoelectrical layers with different resistivities. It consists mainly of the topsoil up to 2 m thick, with a resistivity varying between 49.6 and 1787 Ω.m and a layer of ferrous crust 14.4 m thick with a resistivity up to 4144 Ω.m. The lateritic-clay layer with a thickness of up to 50 m and a resistivity that varies between 58.8 and 970 Ω.m and the fresh rock with resistivity that can reach 100,000 Ω.m (Table 1).

These vertical electrical sounding curves also show that the resistivity can vary within the different layers. These different variations in resistivity within the same layer indicate the heterogeneity of the layer. It can also be seen in Fig.6 that the transition from one layer to another is characterised by a gradual change in resistivity, indicating that there is no abrupt change in facies along the weathering profile. This is particularly evident between the fractured layer and the fresh rock (Fig.6). Thus, this makes it difficult to identify the boundary between these two layers. All these

observations do not allow us to determine with certainty the geometric boundary between the successive layers of the weathering profile.

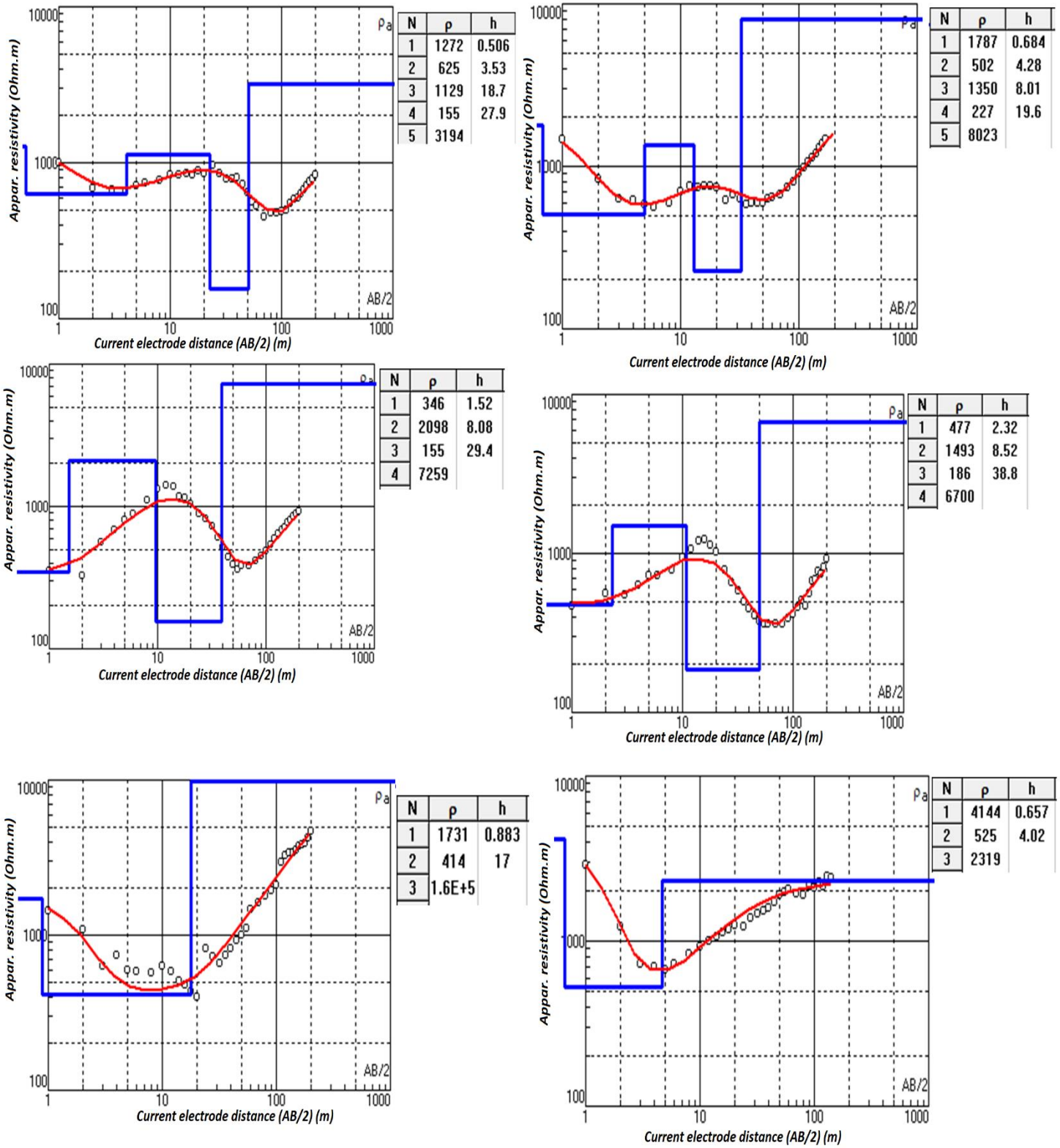

Fig. 5. Some vertical electrical soundings curves carried in the study area

Table 1

Summary of interpretation of results of vertical electrical soundings (VES)

VES n°	Layer thickness (m)				Layer resistivity (Ωm)				
	H1	H2	H3	H4	ρ_1	ρ_2	ρ_3	ρ_4	ρ_5
1	1.5	4.3	27.4	-	538	3902	218	2813	-
2	**0.7**	**4.3**	**8**	**19.6**	**1787**	**502**	**1350**	**227**	**8023**
3	0.6	3.5	18.7	27.9	1272	625	1129	155	3194
4	**0.3**	**7.1**	**6.5**	**19.9**	**841**	**133**	**1450**	**104**	**81493**
5	**1.5**	**8.1**	**29.4**	**-**	**346**	**2098**	**155**	**7259**	-
6	**2.3**	**8.5**	**50.1**	**-**	**477**	**1493**	**186**	**6700**	-
7	1.6	8.4	31.4	-	905	2273	186	6974	-
8	2	6	28	-	467	1787	138	96079	-
9	**1**	**17**	**-**	**-**	**1731**	**414**	**$1.6*10^5$**	-	-
10	2	3.3	38.7	-	528	1248	170	33626	-
11	**0.6**	**4**	**-**	**-**	**4414**	**525**	**2319**	-	-
12	1.3	8.4	25.8	-	1136	1504	123	3981	-
13	2.1	14.1	32.5	-	65.8	697	143	1020	-
14	1	18.8	26.1	-	155	818	183	1749	-
15	0.8	8.3	23.7	-	185	2394	203	2936	-
16	0.8	17.4	30.4	-	49.6	1041	138	5174	-
17	2	25.8	17.4	-	75	856	58.8	1022	-
18	1.1	26.2	26.1	-	83.6	956	95.6	1169	-
19	1.1	18.4	31.7	-	65.2	1204	59.5	946	-
20	1.1	20.1	29.9	-	237	970	86.1	2413	-
21	0.4	14.8	21.4	-	123	1685	133	5666	-
22	1.6	13.6	26.9	-	117	1000	253	1425	-
23	0.3	14.4	34.9	-	120	2006	194	1585	-
24	1.5	9.78	34.5	-	582	2776	458	4580	-
25	0.9	17.1	31.1	-	386	852	216	690	-
26	0.3	12.7	31.9	-	207	1614	179	1752	-
27	1.9	10.5	26.6	-	527	3008	127	2890	-
28	0.7	10.9	26.6	-	234	2987	152	3069	-
29	1.3	11.4	35.9	-	631	1898	256	1128	-
30	1.7	7.5	37.5	-	726	3530	202	1523	-

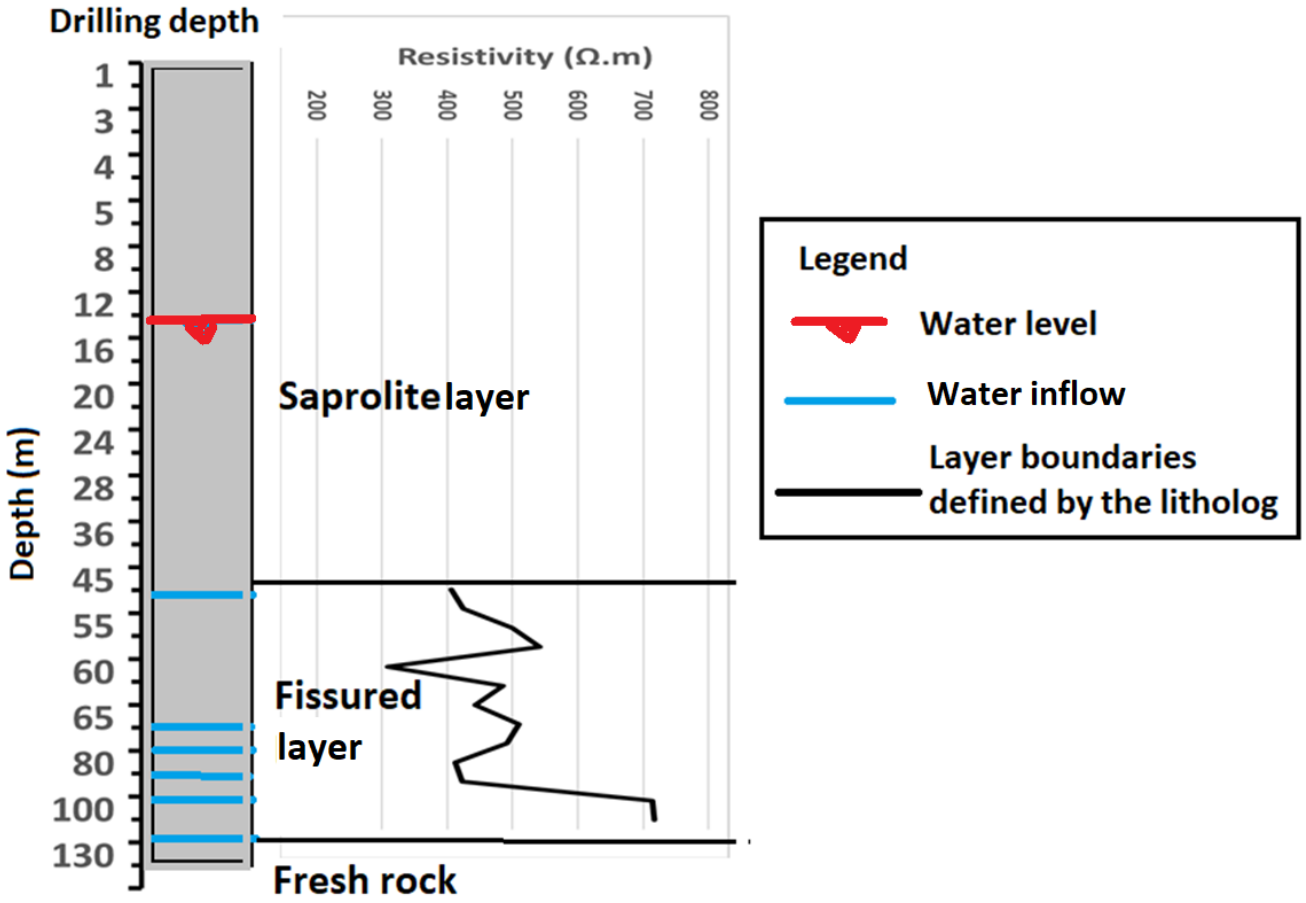

Fig. 6. Variation of electrical resistivity with depth at site 1, drilling

Statistical analysis

Statistical analysis of all the borehole data and the various vertical electrical soundings shows that the median values of electrical resistivity for the "saprolite" layer, the "fissured" layer and the "fresh rock" are 712, 218 and 5420 Ω.m, respectively (Fig.7). Plotting the lower and upper quartiles of resistivity for each layer allows the three main layers of the medium to be distinguished. The lower and higher quartiles 155 Ω.m and 1129 Ω.m, calculated with the VES data, characterise the base of the weathering layer and the fissured layer, respectively. These values were then used to define the boundaries between the three layers: for the 'saprolite', 'fissured' and 'Fresh rock' layers, the following ranges of electrical resistivities were selected: [0 to 155 Ω.m], [155 to 1129 Ω.m] and [1129 to 100,000 Ω.m [. A resistivity threshold of 50 Ω.m was also used to distinguish the most conductive parts of the saprolite. These ranges of resistivities, thus defined, allowed us to propose a geological interpretation for the 2D resistivities measured in our area.

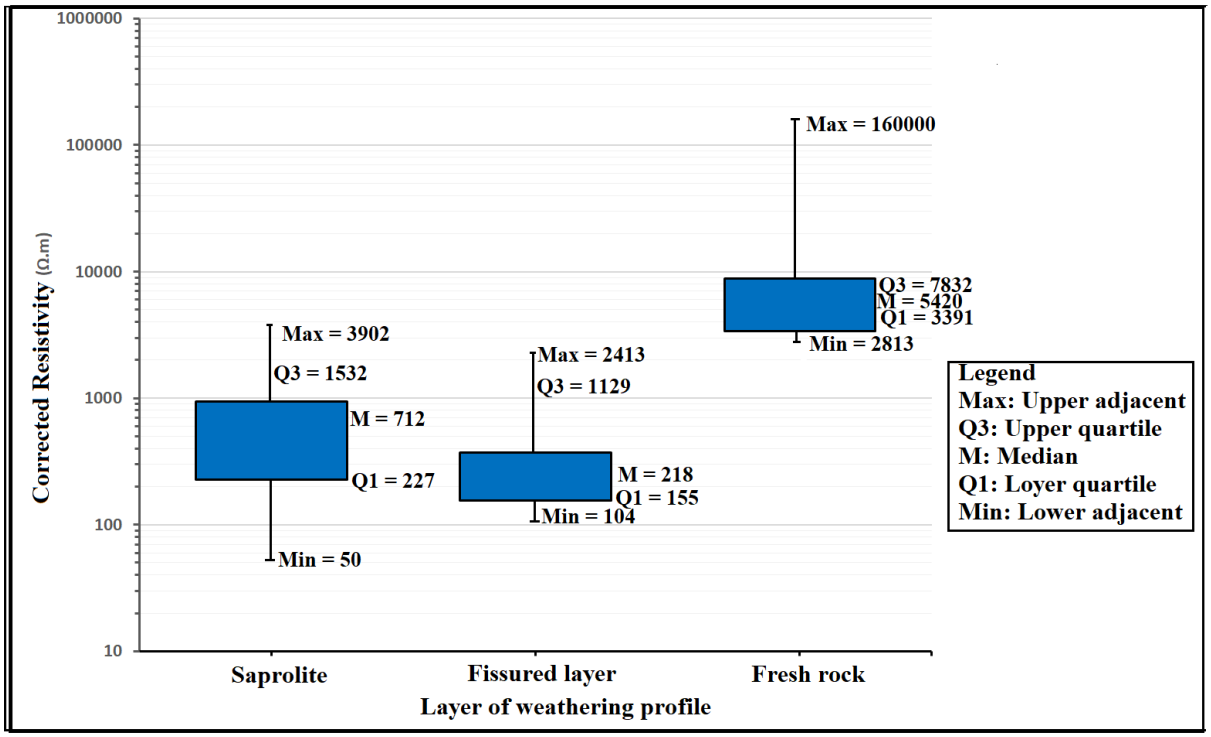

Fig. 7. Grouping resistivities according to the layers of the weathering profile

Geophysical interpretation of ERT data

Fig.8 below shows inverted data representing the profile of this region. High resistivity values with yellow to red colours and low resistivity values with blue and green colours are observed in all profiles. These blue and green colours which are found in all profiles indicate the presence of conductive materials while the others (yellow, orange and red) indicate the presence of resistant materials.

The results of the data inversion show that the highly conductive regions have resistivity values between [50-1129 Ω.m]. These areas may correspond to the saprolite or fissured layer. The resistivity of these zones can in places be lower than 50 Ω.m. These highly conductive areas show a trend of increasing resistivity values with depth. At great depth, resistivity values can sometimes exceed 100,000 Ω.m. These zones correspond to fresh rock.

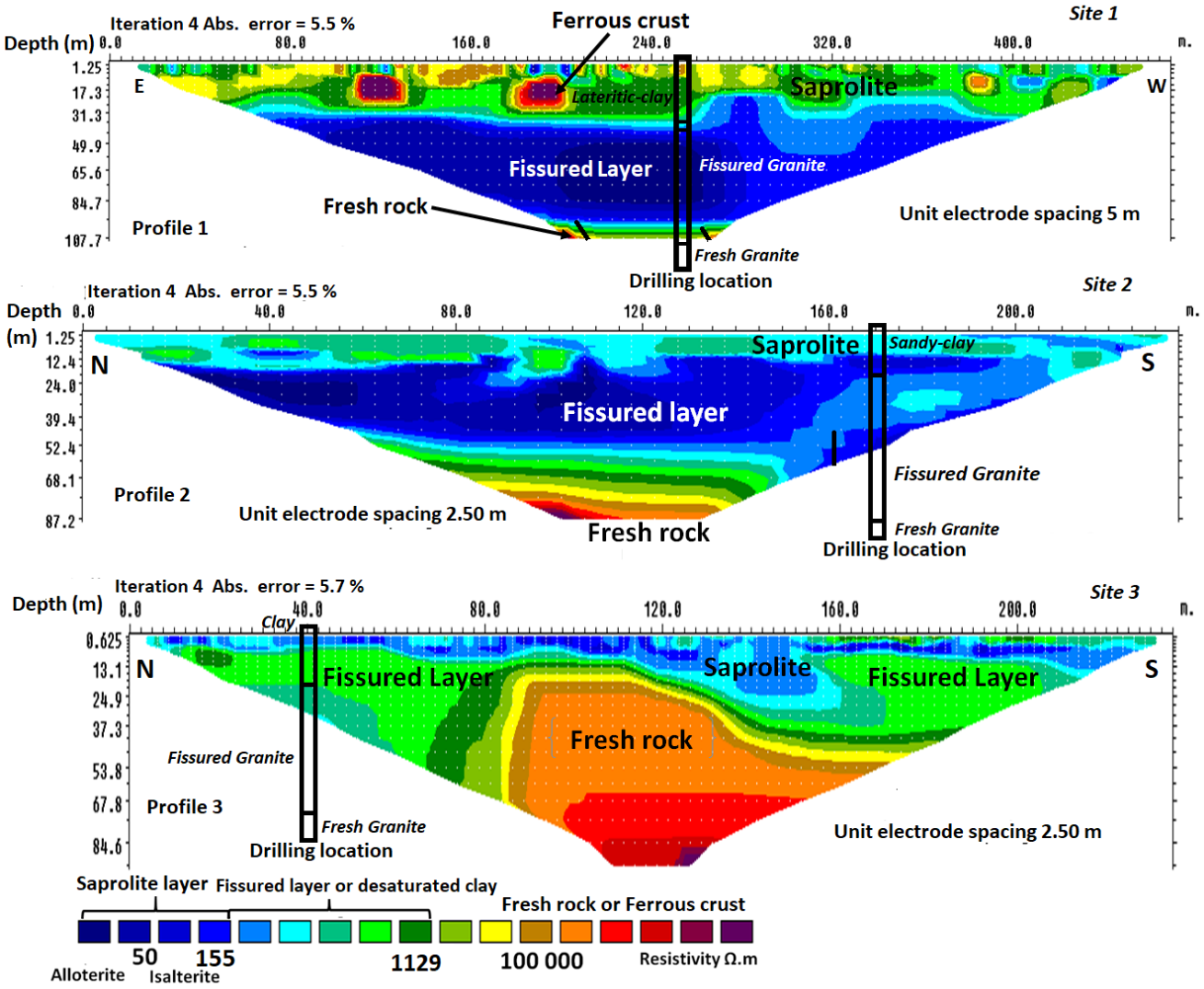

Fig. 8. Classification of interpreted resistivities from the profiles

Hydrogeological interpretation of ERT data

Geologic interpretation of electrical resistivity tomography ERT data has used lithologic information from boreholes in the vicinity of the profile. These profiles generally consist of three layers, sometimes overlain by a thick layer of iron crust, ferruginous in the upper part and clayey in the lower part. From top to bottom we have a layer of saprolite, the thickness of which varies from 21 to 55 m, with an average of 38 m and a resistivity of below 155 Ω.m. This layer is clayey and overlain in places by a thick layer of ferrous crust, about 5 m thick. The fissured layer, ranging in thickness from 35 to 83 m with an average of 68 m and has a resistivity generally ranging from 155 to 1129 Ω.m. In our area, it consists mainly of slightly weathered granite. The underlying fresh rock (beneath the first two layers) is generally at a depth between 93 and 108 m, but in some cases, it can upwell a depth of 13 m or even outcrop. This hydrogeological conceptual model allows us to understand the hydrodynamic function of this aquifer system. Indeed, the presence of ferrous crust in this area could favour the runoff of rainwater towards topographically low points, thus

representing preferential groundwater recharge zones. As for the fractured zone, its productivity depends on its thickness and the density of the fracturing (Fig. 9).

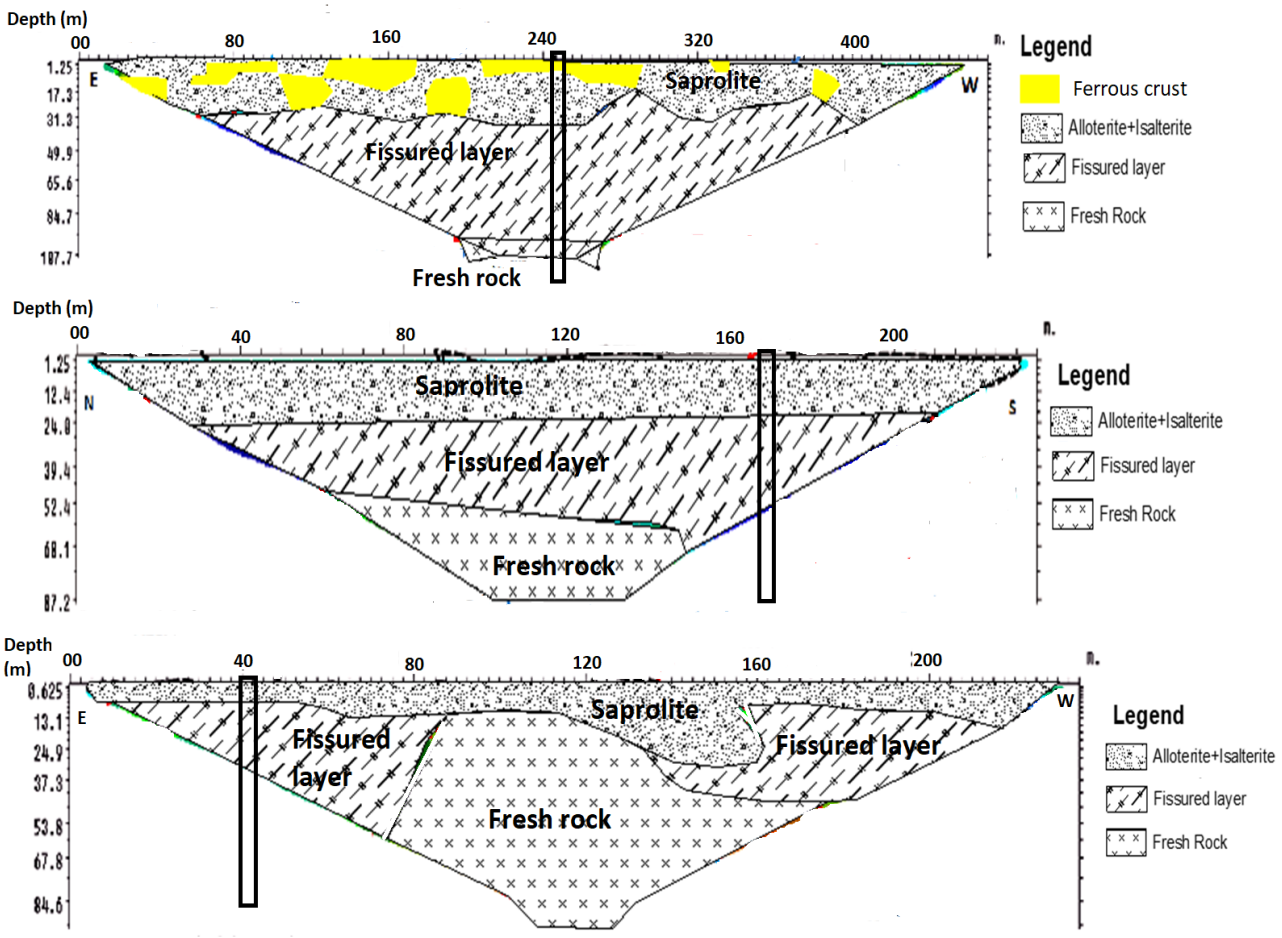

2

278 **Fig. 9.** Geological model of the completed profiles.

279 Discussion

280 Interpretation of the geophysical profiles conducted to map the geometry of aquifer system
281 required knowledge of the general geology of the area. Therefore, several drilling logs were used.
282 This combination of geophysical methods and drilling logs was very useful in mapping the geometry
283 of the aquifers in our area. The weathering profile proposed in this study shows top-down
284 structuring into four main distinct layers as proposed by [29, 30, 13, 4]:

285 The **ferrous crust layer** may be absent, but when present, its average thickness is about 5 m.
286 This layer is ferruginous in the study area. When it is protected from erosion and heavy rainfall
287 recharged, the ferrous crust can give rise to small perched aquifers with locally some springs [30,4].
288 In this area, the resistivity of the ferrous crust is generally above 4000 Ω.m.

289 **The saprolite layer**, this layer originates from the decomposition of the source rock and
290 generally consists of two subunits, the clay-rich alloterite layer and the sand-rich isalerite layer. With
291 an average thickness of about 37 m, generally rich in clay, it can be up to 55 m thick in places. This

layer forms the first level of our composite aquifer. It contains the water table, generally tapped by traditional wells. This saturated layer ensures the capacitive function of the composite aquifer. Due to its low hydraulic conductivity and high porosity [31,32], it is not sustainable. In our area, this layer is largely saturated as the piezometric level is generally 10 m below ground level. This saturated layer could play an important role in recharging deeper aquifers.The resistivity of the clay-dominated saprolite is below 50 Ω.m. The underlying isalerite zone has generally a resistivity from 50 to 155 Ω.m what is higher than the clay layer ones. This geoelectrical description of the saprolite layer is consistent with that proposed by [12,13].

Beneath the saprolite layer, **the fissured** layer, is also called saprock by some authors [33]. This layer is characterized by a very intense fracturing in the first few meters (14.4 m). Its thickness varies from 25 to 63 m and can reach 83 m in places, with water inflow at 118 m. In places where the saprolite has not been eroded, the thickness of the fissured layer is about twice that of the saprolite and can exceed 100 m thick [34,35,36]. The resistivity of the fissured layer ranges from 155 to 1129 Ω.m and can be less than 155 Ω.m in places if it is thick enough. It is the main aquifer in our study zone. For future drilling with high yield, these fractured zones with low resistivity should be searched the most. This description of the proposed fissured layer for the Lobo catchment composite aquifer is consistent with that proposed by [12,16]. Beyond 105 m depth, there is a progressive decrease in the occurrence of water-bearing horizons until 130 m depth where no water-bearing horizon is observed. This progressive decrease in the occurrence of water-bearing horizons with depth, implying an increase in resistivity, shows a decrease in fracture density with depth [37, 31]. These results, based on from the geometry and geological structure of the saprolite layer and the fissured layer, allow us to fix the depth in our area at no more than 130 m. Beyond this depth, high electrical resistivity values are observed, which make fresh rock appear.

The fresh rock is permeable only where "deep fractures are present. Although these fractures are as permeable as fractures in the fissured zone, their density is literally lower with depth [38]. This zone sometimes has resistivity greater than 100,000 Ω.m, which characterizes the underlying fresh rock. For water resources studies in the Lobo catchment, the bedrock is considered impermeable with negligible storativity [37]. The weathering profile of the Lobo catchment has not been previously characterized geologically, hydrogeologically or geophysically. However, this weathering profile highlighted in this study is similar in structure but different in geometry from that developed by [13] in similar formations in Burkina Faso and by [29] in eastern Côte d'Ivoire. In general, resistivity values obtained with ERT techniques and logs of new drillings realized after this study showed good agreement with some differences. As a result of this study, 16 boreholes were realized. The success rate of these boreholes is 69%, i.e., 11 out of 16 wells realized. Boreholes declared as negative are those with a yield ($Q \leq 6\ m^3/h$). The depth of these boreholes varies from 93

to 130 m with an average of 110 m. The average yield of these boreholes is 15.18 m^3/h with a maximum flow rate of 22 m^3/h. Hydraulic investigations carried out in the zone prior to this study, without precise knowledge of the geometry of the underlying aquifer system, have given less satisfactory results. In fact, the average depth of the realized old drillings is 63 m with an average yield of 4.4 m^3/h. This difference could be explained by the lack of knowledge of the geometry of this aquifer system and the hydraulic role of the deep fractures at the time these wells were drilled. Indeed, studies carried out in Côte d'Ivoire on granitic rocks have set the maximum depth of the boreholes at 80 m [39,40]. This lack of knowledge about the geometry of this aquifer system may help to explain the high number of negative boreholes in the study area.

Conclusions

The weathering profile of the Lobo catchment proposed in this study is similar to that proposed in the hard rock in recent years. Thus, from our various analyses, it appears that the alteration profile is a standard one with four main layers: the iron crust, the alteration layer composed of isalerite and alloterite, the fissured layer and the fresh rock. The ferrous crust averages 5 m thick, the saprolite layer is 37 m thick and the fissured layer is 68 m thick but can reach 83 m. In the Lobo catchment, the thicker fissured horizons should be the preferred sites for productive drilling. In general, from 37 m depth, areas with resistivities from 155 to 1129 Ω.m should be preferred targets for future drilling. These results allow us to estimate the optimal drilling depth in this area, i.e., the depth beyond which drilling is not necessary, as the probability of having significant flows decreases. In this study, through analysis of ERT and borehole data, a depth of no more than 130 m was suggested to penetrate as far as possible into the saprolite and fissured layer. The resistivity values obtained in this study will be used as a guide for future investigations. This study provided information on the geometry of the aquifer system in this area. The boreholes drilled following this study, which validated this geometry, have a success rate of about 70% with an average yield of 15.18 m^3/h, which is 4 times higher than the values obtained in previous studies. These results are therefore interesting for the planning and management of groundwater in our area and for the evaluation of the financial costs of hydraulic campaigns (depth of wells to be realized) including preliminary geophysical surveys, which can also be accurately sized. This study was carried out mainly on granitic rocks that cover about 90% of our area. However, similar studies need to be conducted on shale formations to elaborate a typical alteration profile of all the geologic formations in the aquifer system underlying our study. More powerful geophysical methods with even longer cables will have to be used to explore this aquifer system at great depth. An estimate of groundwater recharge should be made to improve the sustainable management of this resource.

Declaration of Competing Interest

The authors declare no conflicts of interest.

Acknowledgments

We would like to thank all those people who helped us in the practical phase of this study

The effort of all the reviewers of this article is greatly acknowledged.

Funding

EPEAEP_Daloa project is funded by the Education and Research Ministry of Côte d'Ivoire, as part of the Debt Reduction-Development Contracts (C2Ds) managed by IRD ».

References

[1] M.T. Youan, T. Lasm, J.P. Jourda, K.F. Kouamé, M. Razack, Cartographie des accidents géologiques par imagerie satellitaire Landsat-7 ETM+ et analyse des réseaux de fractures du socle précambrien de la région de Bondoukou (nord-est de la Côte d´Ivoire). Télédétection 8 (2) (2008) 119–135.

[2] B. Koffi, M. Sanchez, K.L.Kouassi, Z.A. Kouadio, K.H. Kouassi, A.B. Yao, Evaluation of the impacts of climate change and land-use dynamics on water resources: The case of the Lobo River watershed: Central-Western Côte d'Ivoire. EGU General Assembly 2021 Author(s) 2021, EGU21: Gather Online. (2021) 19–30 April 2021. doi.org/10.5194/egusphere-egu21-506

[3] L. Maurice, R.G Taylor, C. Tindimugaya, A.M MacDonald, P. Johnson, A. Kaponda, M.Owor, H. Sanga, H.C. Bonsor, W.G. Darling, D. Gooddy, Characteristics of high-intensity groundwater abstractions from weathered crystalline bedrock aquifers in East Africa. Hydrogeol J. (2018) 27:459. doi.org/10.1007/s10040- 018-1836-9.

[4] P. Lachassagne, B. Dewandel, R. Wyns, Review: Hydrogeology of weathered crystalline/hard-rock aquifers—guidelines for the operational survey and management of their groundwater resources. Hydrogeology. J. (2021) 1-34 doi.org/10.1007/s10040-021-02339-7.

[5] P. Lachassagne, R. Wyns, B. Dewandel, The fracture permeability of hard rock aquifers is due neither to tectonics, nor to unloading, but to weathering processes. Terra Nova. 23 (3) (2011) 145-161. doi.org/10.1111/j.1365-3121.2011.00998.x.

[6] Kamenan, Y.M. Elaboration d'un modèle de protection des eaux souterraines en zone de socle : cas des aquifères du bassin versant de la Lobo à Nibéhibé (Centre-Ouest de la Côte d'Ivoire). Thèse de Doctorat, Université Jean Lorougnon Guédé, Daloa (Côte d'Ivoire). (2021) 170.

[7] A. Duran, Aguas Subterráneas: Investigación aplicada en el abanico aluvial de la cuenca del río Sichez (Groundwater: Applied research in the alluvial fan of the Sichez River watershed). Programa PIAACC. Talleres Gráficos Kipus, Cochabamba. (2018).

[8] C.H. Bakundukize, M.J. Enok, K. Martens, C.M. Van, K. Walraevens, Poor understanding of the hydrogeological structure is a main cause of hand-dug wells failure in developing countries: a case study of a Precambrian basement aquifer in Bugesera region (Burundi). J Afr Earth Sci, (121) (2016) 180–199.

[9] S. Vassolo, C. Neukum, C. Tiberghien, M. Heckmann, K. Hahne, D. Baranyikwa, Hydrogeology of a weathered fractured aquifer system near Gitega, Burundi. Hydrogeology J. (27) (2019) 625–637. doi.org/10.1007/s10040-018-1877-0.

[10] C.P. Chandra, Groundwater of Hard Rock Aquifers of India. Groundwater of South Asia, Springer. Hydrogeology. J. (2018) doi.org/10.1007/978-981-10-3889-1_5.

[11] A.G. Amaya, J. Ortiz, A. Duran, M. Villazon, Hydrogeophysical methods and hydrogeological models: basis for groundwater sustainable management in Valle Alto (Bolivia). Sust.Water. Rescs.Management. (2019). doi.org/10.1007/s40899-018-0293-x.

[12] P. Belle, P. Lachassagne, F. Mathieu, N. Brisset, C. Barbet, F. Bonneval, J.C. Gourry, Geological and hydrogeological interpretation of hard rock weathering profil from electrical tomography. In: Ofterdinger U, Macdonald AM, Comte JC, Young ME (eds) Groundwater in fractured bedrock environments. Geol.Soc.Lond.Spec.Publ. (479) (2017). doi.org/10.1144/SP479.7.

[13] D.D Soro, M. Koïta, C.A Biaou, E. Outoumbe, J.M. Vouillamoz, Y. Hamma, R. Guerin, Geophysical demonstration of the absence of correlation between lineaments and hydrogeologically usefull fractures: Case study of the Sanon hard rock aquifer (Central northern Burkina Faso). J. Afri. Earth. Sci. (129) (2017) 842-852.

[14] Q. Gao, Y. Shang, M. Hasan, W. Jin, P. Yang, Evaluation of a Weathered Rock Aquifer Using ERT Method in South Guangdong, China. Water. 10 (293) (2018) 1-22. doi.org/10.3390/w10030293.

[15] S.K. Sandberg, L.D. Slater, R. Versteeg, An integrated geophysical investigation of the hydrogeology of an anisotropic unconfined aquifer. Hydrol. J. (267) (2002) 227–243.

[16] I.C. Alle, M. Descloitres, J.M Vouillamoz, N. Yalo, F.M.A. Lawson, A.C. Adihou, Why 1D Electrical Resistivity Techniques Can Result in Inaccurate Siting of Boreholes in Hard Rock Aquifers and Why Electrical Resistivity Tomography Must Be Preferred: The Example of Benin, West Africa. J. Afr. Earth Sci. (139) (2018) 341-353.

[17] N.Y. Akokponhoué, N. Yalo, B.H. Akokponhoué, R. Houngue, G. Agbahoungba, Contribution of Electrical Resistivity Tomography and Boring Technique in the Realization of Ten (10) Large Boreholes in a Crystalline Basement Rocks in the Centre-West of Benin. J. Geosce. Environ. Protec. (7) (2019) 114-130. doi.org/10.4236/gep.2019.79009.

[18] INS- Institut National de la Statistique. Recensement général de la population et de l'habitat de Côte d'Ivoire. Rapport de synthèse, volume des fiches monographiques des localités : région du Haut-Sassandra. INS Abidjan. (2014) 50.

[19] Tagini B. Esquisse structurale de la Côte d'Ivoire. Essai de géotectonique régionale. Thèse de Doctorat 3ème cycle, Université de Lausanne (Suisse) Bulletin SODEMI. (5) (1971) 302.

[20] O. Massing, I. Adoum, H. Abderamane, N. Dingamnodji, Role of remote sensing and geophysics to determine potential sites for boreholes in the crystalline basement of the wadi fira region: case study of iriba. Asian J. Sci. Technol. 8 (12) (2017) 7073–7082.

[21] S. Bakkali, B.J. Jaâfar, Contribution of the geoelectrical prospection applied to the data of the hydraulic resources of the anergui people (Tafraoute, Moroccan Antiatlas). e-Gnosis. (3) (2005) 1–12. http://www.egnosis.udg.mx/index.php/egnosis/article/viewFile/38/37.

[22] D. Kumar, V. Anand, V.A. Rao, V.S Sharma, Hydrogeological and geophysical study for deeper groundwater resource in quartzitic hard rock ridge region from 2D resistivity data. J. Earth Syst. Sci. (123) (2014) 531–543.

[23] S. Szalai, A. Novak, L.Szarka, Which geoelectric array sees the deepest in a noisy environment? Depth of detectability values of multielectrode systems for various two-dimensional models. Phys. Chem. Earth. (36) (2011) 1398–1404.

[24] J. Bernard, O. Leite, F. Vermeersch, Multi-electrode resistivity imaging for environmental and mining applications. (2006). http://www.iris-instrument.com.

[25] M.H. Loke, RES2DINV, Ver. 3.50, Rapid 2-D resistivity and IP inversion using the least square method. (2002).

[26] M.H. Loke, R.D. Barker, Rapid least-squares inversion of apparent resistivity pseudosections using a quasi-Newton method. Geophys Prospect. (44) (1996) 131–152.

[27] M. Descloitres, O. Ribolzi, Y.L. Troque, J.P Thiebaux, Study of water tension differences in heterogeneous sandy soils using surface ERT. J. Appl. Geophys. (64) (2008) 83-98. doi.org/10.1016/j.jappgeo.2007.12.007.

[28] A. Chaudhuri, M. Sekhar, M. Descloitres, Y Godderis, L. Ruiz, J.J. Braun, Constraining complex aquifer geometry with geophysics (2D ERT and MRS measurements) for stochastic modeling of groundwater flow. J. Appl. Geophys. (98) (2013) 288-297. doi.org/10.1016/j.jappgeo.2013.09.005.

[29] M. Koïta, H. Jourde, K.J.P. Koffi, K.S.D. Silveira, A. Biaou, Characterization of weathering profile in granites and volcano sedimentary rocks in West Africa under humid tropical climate conditions. Case of the Dimbokro Catchment (Ivory Coast). J.Eth. Syst.Sce. 122 (3) (2013) 841–854.

[30] A. Bon, N.J. Ndam, M.G. Ewodo, G. Ekodeck, Hydrogeological characterization of weathered and fissured basement aquifers of the Olezoa watershed in Yaoundé, Cameroon. Rev. sces. Eau. 29 (2) (2016) 149–166. doi :10.7202/1036545ar.

[31] B. Dewandel, P. Lachassagne, R. Wyns, J.C. Maréchal, N.S. Krishnamurthy, A generalized 3-D geological and hydrogeological conceptual model of granite aquifers controlled by single or multiphase weathering. J. hydrology. (330) (2006) 260–284.

[32] A.Boisson, N. Guihéneuf, J. Perrin, O. Bour, B. Dewandel, A. Dausse, M. Viossanges, S. Ahmed, J.C. Maréchal, Determining the vertical evolution of hydrodynamic parameters in weathered and fractured south Indian crystalline-rock aquifers: insights from a study on an instrumented site. Hydrogeol J. 23 (4) (2015) 757–773. doi.org/10.1007/s10040-014-1226-x.

[33] L. Riber, H. Dypvik, R. Sorlie, Comparison of deeply buried paleoregolith profiles, Norwegian North Sea, with outcrops from southern Sweden and Georgia, USA: implications for petroleum exploration. Palaeogeogr Palaeoclimatol Palaeoecol, (471) (2017) 82– 95. doi.org/10.1016/j.palaeo.2017.01.043.

[34] B. Dewandel, M. Alazard, P. Lachassagne, V. Bailly-Comte, R. Couëffé, S. Grataloup, B. Ladouche, S. Lanini, J.C. Maréchal, R. Wyns, Respective roles of the weathering profile and the tectonic fractures in the structure and functioning of a crystalline thermomineral carbo-gaseous aquifer. J. Hydrol. (547) (2017) 690–707.doi. org/10.1016/j.jhydrol.2017.02.028.

[35] R. Wyns, Weathering and lithosphere geodynamics. Géochronique. (1) (2020a) 70–80.

[36] R. Wyns, Weathering paleoprofiles in Vosges and their applications. Bull. Inf. Géol. Bass. Paris, 57 (4) (2020b) 13–27.

[37] J.C. Maréchal, B. Dewandel, K. Subrahmanyak, Use of hydraulic tests at different scales to characterize fracture network properties in the weathered-fractured layer of a hard rock aquifer, Water. Rescs. Resch. (40) (2004) W11508. doi: 10.1029/2004WR003137.

[38] M. Cho, Y.Choi, K.Ha, W.Kee, P. Lachassagne, R.Wyns, Relationship between the permeability of hard rock aquifers and their weathering, from geological and hydrogeological observations in South Korea. International Association of Hydrogeologists IAH Conference on Groundwater in fractured rocks, Prague. (2003) 15–19.

[39] Y.A. N'Go, D.L.Goné, I.Savané, M.M. Goble, Potentialité en eaux souterraines des aquifères fissurés de la région d'Agboville (Sud-ouest de la Côte d'Ivoire): Caractérisation hydro climatique et physique », Afr. Scs. 01 (1) (2005) 127-144.

[40] M.J. Mangoua, S. Touré, B.T.Goula, K.B.Yao, I.Savané, J. Biémi, Evaluation des caractéristiques des aquifères fissurés du bassin versant de la Baya ou Bâ (Est de la Côte d'Ivoire), Rev. Ivoir. Scs. Tech. (16) (2010), 243-259.